Neurobiology of Aging 73 (2019) 30–40

Contents lists available at ScienceDirect

Neurobiology of Aging

journal homepage: www.elsevier.com/locate/neuaging

Aging alters envelope representations of speech-like sounds in the inferior colliculus

Aravindakshan Parthasarathy [a,b,1], Björn Herrmann [c,1], Edward L. Bartlett [a,*]

[a] Departments of Biological Sciences and Biomedical Engineering, Purdue University, West Lafayette, IN, USA
[b] Department of Otolaryngology, Harvard Medical School, and Eaton-Peabody Laboratories, Massachusetts Eye and Ear Infirmary, Boston, MA, USA
[c] Department of Psychology & Brain and Mind Institute, The University of Western Ontario, London, Ontario, Canada

ARTICLE INFO

Article history:
Received 28 March 2018
Received in revised form 13 August 2018
Accepted 27 August 2018
Available online 12 September 2018

Keywords:
Inferior colliculus
Voice onset time
Evoked potentials
Hearing loss

ABSTRACT

Hearing impairment in older people is thought to arise from impaired temporal processing in auditory circuits. We used a systems-level (scalp recordings) and a microcircuit-level (extracellular recordings) approach to investigate how aging affects the sensitivity to temporal envelopes of speech-like sounds in rats. Scalp-recorded potentials suggest an age-related increase in sensitivity to temporal regularity along the ascending auditory pathway. The underlying cellular changes in the midbrain were examined using extracellular recordings from inferior colliculus neurons. We observed an age-related increase in sensitivity to the sound's onset and temporal regularity (i.e., periodicity envelope) in the spiking output of inferior colliculus neurons, relative to their synaptic inputs (local field potentials). This relative enhancement for aged animals was most prominent for multi-unit (relative to single-unit) spiking activity. Spontaneous multi-unit, but not single-unit, activity was also enhanced in aged compared with young animals. Our results suggest that aging is associated with altered sensitivity to a sound's temporal regularities, and that these effects may be due to increased gain of neural network activity in the midbrain.

1. Introduction

Older and middle-aged listeners experience difficulties understanding speech, particularly in challenging listening situations such as in the presence of background sounds, competing speakers, or reverberation (Pichora-Fuller and Souza, 2001; Ruggles et al., 2011). Speech perception depends on the sensitivity of the auditory system to temporal regularities in sounds. Temporal regularities in speech may be divided into 3 categories: the slow fluctuations (<50 Hz) of the speech envelope that capture word and syllabic rate; the periodicity envelope (50–500 Hz), which contains the fundamental frequency of the speaker's voice (f0) and is crucial for speaker identification (Bregman, 1990); and the temporal fine structure (>500 Hz), which contains information about formant structure (Rosen, 1992). The sensitivity of the auditory system to temporal regularity in sounds declines with age, with drastic consequences for speech perception (Anderson et al., 2011; Fullgrabe et al., 2015; Walton, 2010), but the neurophysiological changes that underlie this age-related decline are not well understood.

An age-related decline in temporal processing abilities is thought to be primarily neural in origin because it is independent of changes in hearing thresholds due to impaired cochlear function (Frisina and Frisina, 1997; Gordon-Salant and Fitzgibbons, 2001; Pichora-Fuller and Souza, 2001). The neural deficits that may contribute to impaired sensitivity to temporal regularity include cochlear synaptopathy—that is, the degradation of cochlear synapses between inner hair cells and auditory nerve fibers (Sergeyenko et al., 2013)—and a decrease in inhibitory neurotransmitters in the brainstem, midbrain, and cortex (Caspary et al., 2008; Rabang et al., 2012; Takesian et al., 2009). Loss of inhibition may result in increased neural activity in central auditory regions despite diminished inputs from peripheral structures (Hughes et al., 2010; Mohrle et al., 2016; Parthasarathy et al., 2014; Parthasarathy and Kujawa, 2018). However, it is less clear how aging affects sensitivity to temporal regularity in central auditory regions, in particular for complex, speech-like sounds.

Previous work suggests that neurons in the inferior colliculus show altered temporal processing including changes in the sensitivity to the temporal regularities in sounds (Palombi et al., 2001; Rabang et al., 2012; Schatteman et al., 2008; Walton et al., 1998, 2002). These studies focused on neuronal spiking, which reflects the output of neurons. By contrast, local field potentials (LFPs) are thought to reflect the summed synaptic inputs to a neuron or local

* Corresponding author at: 206 S. Martin Jischke Drive, West Lafayette, IN, 47906, USA. Tel.: +1 765 496 1425.
E-mail address: ebartle@purdue.edu (E.L. Bartlett).
[1] Aravindakshan Parthasarathy and Björn Herrmann contributed equally to this work.

0197-4580/$ – see front matter © 2018 Elsevier Inc. All rights reserved.
https://doi.org/10.1016/j.neurobiolaging.2018.08.023

neuronal population to a large degree (but other nonsynaptic activity might additionally contribute [Bullock, 1997; Buzsaki et al., 2012; Logothetis et al., 2001; Logothetis and Wandell, 2004]). Recent recordings of LFPs and spiking activity show that synchronization of spiking activity (output) is abnormally enhanced in the aging inferior colliculus, despite decreased synaptic inputs (input), and that this age-related relative increase in activity (i.e., from a neuron's input to its output) is specific for sounds with modulation rates below 100 Hz (Herrmann et al., 2017). Whether aging also leads to an oversensitivity to temporal regularities in complex, speech-like sounds is unknown.

In the present study, we test the hypothesis that neural synchronization to the periodicity envelope (~100 Hz) of speech is abnormally enhanced in the inferior colliculus of aged animals. We assess peripheral neural function by measuring wave 1 amplitudes of the auditory brainstem responses (ABRs) and show physiological evidence for cochlear synaptopathy in aged animals. Scalp-recorded neural synchronization to the envelope of a speech-like stimulus is increased specifically in more rostral regions in the auditory pathway such as the inferior colliculus compared with more caudal ones such as the auditory nerve. Furthermore, we assess the relation between LFPs (synaptic input) and spiking output in the inferior colliculus using extracellular recordings. Synchronization of LFPs to the envelope of a speech-like sound is decreased in aged animals, whereas synchronization of spiking activity from well isolated units does not differ between age groups. Multi-unit spike synchronization, however, is drastically increased for aged animals, suggesting changes in gain control mechanisms occurring largely at a neural network level.

2. Methods and materials

2.1. Ethical approval

The experimental procedures described in the present investigation were approved by the Institutional Animal Care and Use Committee of Purdue University (PACUC #1111000167). The experiments included in this study comply with the policies and regulations described by (Drummond, 2009). Rats were housed 1 per cage in accredited facilities (Association for the Assessment and Accreditation of Laboratory Animal Care) with food and water provided *ad libitum*. The number of animals used was reduced to the minimum necessary to allow adequate statistical analyses.

2.2. Subject population

The study design is cross-sectional and used male Fischer-344 rats obtained from Charles River Laboratories and Taconic. The aging Fisher-344 rat has been suggested to be a suitable model to study presbycusis in aging animals (Syka, 2010) and has been shown to exhibit high-frequency hearing loss and metabolic presbycusis that are characteristic of human age-related loss of hearing sensitivity (Allen and Eddins, 2010; Dubno et al., 2013). Eleven young (3–6 months, ~300 g) and 12 aged (22–26 months, ~400–500 g) animals were used for scalp recordings, and 11 young (3–6 months, ~300 g) and 9 aged (22–26 months, ~400–500 g) animals were used for extracellular recordings. A subset of the ABR recordings have been reported in previous studies (Parthasarathy and Bartlett, 2012; Parthasarathy et al., 2014).

2.3. Sound stimulation

The stimulus was a natural English syllable, /ba/, which was 260 ms long and spoken by a male speaker of North American English with a fundamental frequency of ~110 Hz. To account for the differences in the hearing range between rats and humans, as well as to increase the number of responsive neurons in the inferior colliculus of rats, this speech token was half-wave rectified, and used to modulate a broadband noise carrier (0.04–40 kHz) (Fig. 1A). This preserved the periodicity envelope as well as the original fine structure of the speech token, both of which served as the modulator for the broadband noise (Fig. 1B and C). This stimulus design was chosen to understand how neurons represent temporal regularities that are important for human speech and to aid comparison with human literature, rather than investigating the representation of conspecific vocalizations that may not generalize to human speech processing.

2.4. Stimulus generation

Sound stimuli were generated using SigGenRP (Tucker-Davis Technologies [TDT]) sampled at a rate of 97.64 kHz (standard TDT sampling rate) and presented through custom-written interfaces in OpenEx software (TDT). Sound waveforms were generated via a multichannel processor (RX6, TDT), amplified (SA1, TDT), and presented free field through a Bowers and Wilkins DM601 speaker. The output from the speaker was calibrated free field, using SigCal (TDT) and a Bruel & Kjaer microphone with a 0.25-in. condenser, pointed at frontal incidence to the speaker, from the same location as the animal's right ear, and was found to be within ±6 dB for the frequency range tested. All recordings took place in an Industrial Acoustics booth lined with 1 inch (35 mm) Sonex foam with ~90% absorption for frequencies ≥1000 Hz, minimizing potential echoes and reverberations. All analyses described below accounted for the travel time of the sound wave from the speaker to the animals' ears.

2.5. Electrophysiological recordings at the scalp

Methods for experimental setup, sound stimulation, and scalp-potential recordings are similar to those described before (Parthasarathy et al., 2014, 2016). The animals were briefly anesthetized using isoflurane (1.5%–2%) for the insertion of subdermal needle electrodes (Ambu) and the intramuscular injection of dexmedetomidine (Dexdomitor, 0.2 mg/kg), an α-adrenergic agonist that acts as a sedative and an analgesic. Recordings commenced

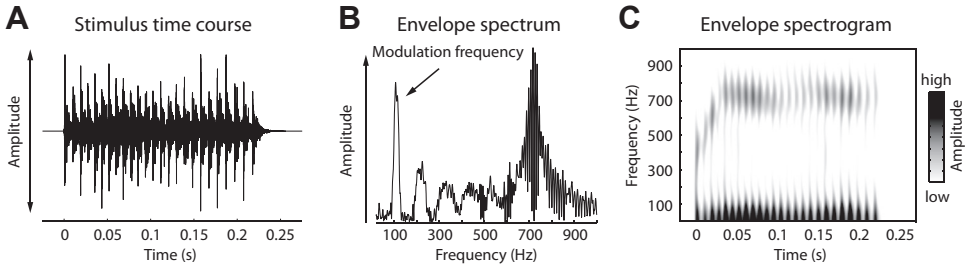

Fig. 1. Speech-like sound used in the present study. (A) Waveform of the speech-like sound. (B) Amplitude spectrum of the envelope of the speech-like sound displayed in panel A. (C) Spectrogram of the envelope of the speech-like sound.

after a 15-minute recovery from the anesthesia and were terminated if the animal showed any signs of discomfort such as increased breathing or major movement as monitored by a video camera in the recording chamber.

The scalp-evoked responses to the temporal envelope of the speech-like sound (envelope following response [EFR]) were obtained using 2 simultaneous recording channels. One positive electrode (caudal channel) was placed on the animal's forehead along the midline at Cz–Fz. This electrode has a strong wave 3 ABR component (cochlear nuclei) and best sensitivity to modulation frequencies $\geq$100 Hz (Parthasarathy and Bartlett, 2012). Another positive electrode (rostral channel) was placed horizontally, along the interaural line, above the location of the inferior colliculus. This electrode has a strong wave 1, 4, and 5 ABR components (auditory nerve, the inferior colliculus, and its afferents) and best sensitivity to modulation frequencies $<$100 Hz (Parthasarathy and Bartlett, 2012). The negative electrode was placed under the right ear, along the mastoid, and the ground was placed in the nape of the neck. Impedances were ensured to be always less than 1kΩ as tested using the low-impedance amplifier (RA4LI, TDT).

This two-channel setup allowed greater sensitivity to different ranges of modulation frequencies and putative generators compared with recording from a single channel alone, as reported previously (Parthasarathy and Bartlett, 2012). Signal presentation and acquisition were performed by BioSig software (TDT). The stimulus was presented free field to the right of the animal, at a distance of 115 cm from speaker to the right ear. Digitized waveforms were recorded with a multichannel recording and stimulation system (RZ-5, TDT) and analyzed with BioSig and custom-written programs in MATLAB (Mathworks).

2.6. Surgical procedures for extracellular recordings

Methods for surgery, sound stimulation, and recording are similar to those described in (Herrmann et al., 2015; Rabang et al., 2012). Surgeries and recordings were performed in a 9′×9′ double-walled acoustic chamber (Industrial Acoustics Corporation). Animals were anesthetized using a mixture of ketamine (VetaKet, 80 mg/kg) and dexmedetomidine (Dexdomitor, 0.2 mg/kg) administered intramuscularly via injection. A constant physiological body temperature was maintained using a water-circulated heating pad (Gaymar) set at 37°C with the pump placed outside the recording chamber to eliminate audio and electrical interferences. The animals were maintained on oxygen through a manifold. The pulse rate and oxygen saturation were monitored using a pulse-oximeter to ensure they were within normal ranges during surgery. Supplementary doses of anesthesia (20 mg/kg of ketamine, 0.05 mg/kg of dexmedetomidine) were administered intramuscularly as required to maintain areflexia and a surgical plane of anesthesia. An initial dose of dexamethasone and atropine was administered before incision to reduce swelling and mucosal secretions. A subdermal injection of Lidocaine (0.5 mL) was administered at the site before the first incision. A central incision was made along the midline, and the calvaria exposed. A stainless steel headpost was secured anterior to bregma using an adhesive and 3 screws drilled into the skull to provide structural support for a head cap, constructed of orthodontic resin (Dentsply). A craniotomy was performed from 9–13 mm posterior to bregma, which extended posterior to the lambda suture, and 3-mm wide extending from the midline. The dura mater was kept intact, and the site of recording was estimated stereotaxically using a rat atlas (Paxinos and Watson, 2006) as well as using internal vasculature landmarks and physiological measurements. At the completion of recordings, animals were euthanized with Beuthanasia (200 mg/kg IP). Once areflexive, they were perfused transcardially with 150–200 mL phosphate buffered saline followed by 400–500 mL 4% paraformaldehyde. The brain was then removed and stored or processed further for Nissl or immunohistochemistry.

2.7. Electrophysiological recordings in extracellular space

Neural activity in inferior colliculus was recorded in vivo using a tungsten microelectrode (A-M Systems) encased in a glass capillary that was advanced using a hydraulic microdrive (Narishige). We recorded 118 units in young rats and 121 units in aged rats. The inferior colliculus was identified based on short-latency–driven responses to tone stimuli. The central nucleus of the inferior colliculus was identified using the ascending tonotopy moving in a dorsoventral direction as well as narrowly tuned responses to pure tones with frequencies ranging from 0.5 to 40 kHz. Recordings were obtained from both the dorsal cortex and central nucleus. Although we cannot exclude that we recorded from dorsal and lateral (or external) cortex, based on the recording depth, the presence of sustained responses to tones and amplitude-modulated stimuli, as well as clear frequency tuning in most cases, we estimate that most of our units were recorded from the central nucleus.

The sounds were presented to the animal at azimuth 0° and elevation 0°. Neural signals were acquired using the tungsten microelectrode connected to a headstage (RA4, TDT) and were amplified (RA4PA preamplifier, TDT). The digitized waveforms and spike times were recorded with a multichannel recording and stimulation system (RZ-5, TDT) at a sampling rate of 24.41 kHz (standard TDT sampling rate). The interface for acquisition and spike sorting were custom-made using the OpenEx and RPvdsEx software (TDT). The units acquired were filtered between 500 Hz (occasionally 300 Hz) and 5000 Hz. The acquired spikes were stored in a data tank and analyzed using custom-written software in MATLAB. LFPs were simultaneously recorded from the same electrode by sampling at 1525.88 Hz and bandpass filtering from 3 to 500 Hz.

2.8. Assessment of peripheral and brainstem function

ABRs were recorded using the scalp-recording setup described previously. ABRs were recorded in response to brief broadband click stimuli of 0.1-ms duration that varied in sound level from 5 to 95 dB sound pressure level (SPL) in 10 dB steps. The stimuli were presented in alternating polarity at 26.6 clicks per second. The acquisition window was 20 ms, and each ABR was an average of 1500 repetitions. The ABR amplitudes of different waves were calculated as the amplitude of the peak of the wave from the baseline, in BioSig (TDT). The differences in thresholds between young and aged Fisher-344 rats have been reported previously (Parthasarathy et al., 2014) and correspond to ~15–20 dB loss using broadband clicks. Hence, ABRs between groups were compared at peak response level, which was determined as the lowest sound level that produced the maximum amplitude for each animal. This typically corresponded to 70–75 dB SPL for the young and 80–85 dB SPL for the aged rats.

2.9. Analysis of neural synchronization recorded at the scalp

For scalp-recorded neural synchronization (i.e., EFRs), the speech-like stimulus (described previously) was presented with a repetition rate of 3.1 Hz (leading to an interstimulus interval of 63 ms). Although the interstimulus interval is relatively short (63 ms), we did not expect spill-over effects from one stimulus presentation to the next as the timescale for recovery of forward masking at the auditory nerve, cochlear nucleus, superior olivary complex, and the inferior colliculus in rodents has been estimated to be within 30–50 ms (Gao and Berrebi, 2016; Ingham et al., 2016;

Snyder and Schreiner, 1985; Verschooten et al., 2012). Furthermore, the interstimulus interval in previous investigations of the effects of age on EFRs in humans used only slightly longer intervals ranging from 80 to 100 ms (Anderson et al., 2012; Schoof and Rosen, 2016). The stimulus was presented at peak response level described previously, which was determined following a fast Fourier transform (FFT) of the time-domain response. Each response time course was obtained as an average of 200 stimulus repetitions in alternating polarity. Responses were filtered online between 30 and 3000 Hz with a 60-Hz notch filter.

To analyze the fidelity of the auditory system to synchronize with the temporal structure in the speech-like sound, we first used a broad-scale approach by calculating the correlation between the stimulus waveform and the response time course for lags ranging from 0 to 0.05 seconds. This cross-correlation approach was calculated twice, once for a low-frequency range (i.e., stimulus waveform and response time course were low-pass filtered at 300 Hz; Butterworth) and once for a high-frequency range (i.e., stimulus waveform and response time course were band-pass filtered from 300 to 3000 Hz; Butterworth). The former assessed neural synchronization to the vowel-like envelope periodicity, the latter assessed neural synchronization to the temporal fine structure in the stimulus. The highest correlation value (out of all lags) was used as a measure of synchronization strength. Separately for the 2 channels and the 2 filtered signals, Wilcoxon's rank-sum test (MATLAB: ranksum) was used to test whether correlation values differed between age groups.

We further investigated neural synchronization by calculating the amplitude spectrum (using an FFT; Hann window; zero-padding) of the averaged time-domain signal. Neural synchronization could not be quantified as intertrial phase coherence (Lachaux et al., 1999) because the recordings were averaged across trials online. This analysis focused on neural synchronization to the envelope of the speech-like sound (~ 110 Hz) and we thus averaged the spectral amplitudes in the frequency window ranging from 105 to 115 Hz. Wilcoxon's rank-sum test (MATLAB: ranksum) was used to test whether neural synchronization to the envelope differed between age groups (separately for the caudal and rostral channel).

2.10. Analysis of local field potentials

LFPs previously band-pass filtered between 3 and 500 Hz during acquisition were further notch filtered at 60 Hz and 120 Hz (elliptic filter; infinite-impulse response [IIR]; zero-phase lag) to suppress line noise and low-pass filtered at 200 Hz (Butterworth; IIR; zero-phase lag).

For the time-domain analysis, single-trial time courses were averaged separately for each age group. Onset responses were analyzed by calculating the root mean square (RMS) amplitude of the averaged signal in the 0–0.08 seconds time window. Wilcoxon's rank-sum test (MATLAB: ranksum) was used to test differences in sound-onset responses between age groups.

Neural synchronization was analyzed by calculating a normalized vector strength spectrum (Herrmann et al., 2017; Wolff et al., 2017). To this end, for each trial, an FFT (Hann window; zero-padding) was calculated using the data ranging from 0.08 seconds to 0.225 seconds after sound onset (frequency range: 20–180 Hz; step size: 0.05 Hz; zero-padding) to exclude onset and offset transients. An intertrial phase coherence (ITPC) spectrum was calculated using the complex values from the FFT (Lachaux et al., 1999). An ITPC permutation distribution was generated by flipping the sign of a random subset of trials (Wolff et al., 2017), followed by ITPC calculation. This procedure was repeated 200 times and resulted in a permutation distribution of ITPC values. The spectrum of normalized vector strength was calculated by subtracting the mean ITPC of the permutation distribution from the empirically observed ITPC and dividing the result by the standard deviation of the permutation distribution (separately for each frequency). The normalized ITPC (vector strength) reflects a statistical measure—that is, a z-score—with a meaningful zero that indicates nonsynchronized activity.

To test for differences in neural synchronization at the envelope frequency between age groups, the normalized vector strength was averaged across the 105–115 Hz frequencies. Wilcoxon's rank-sum test (MATLAB: ranksum) was used to test whether neural synchronization differed between age groups.

2.11. Analysis of multi-unit activity

Multi-unit activity (MUA) was extracted based on the recorded broadband neural signal (Lakatos et al., 2005, 2013). To this end, the signal was high-pass filtered at 300 Hz (Butterworth; IIR; zero-phase lag), full-wave rectified by calculating absolute values, low-pass filtered at 200 Hz (Butterworth; IIR; zero-phase lag), and down-sampled to the sampling frequency of the LFP (1525.88 Hz). Data analysis followed closely the analysis of LFP data.

For the time-domain analysis, single-trial time courses were averaged separately for each age group. Onset responses were analyzed by calculating the mean amplitude of the averaged signal in the 0–0.08 seconds time window. Wilcoxon's rank-sum test (MATLAB: ranksum) was used to test differences in sound-onset responses between age groups.

Neural synchronization was analyzed by calculating a normalized vector strength spectrum using the same procedure as described for the LFP data.

2.12. Analysis of single-unit activity

Overall, we recorded from 89 single units in young, and 123 single units in the aged animals. Single-unit activity (SUA) was isolated online during the recordings of the neural signals. Units that were substantially above noise threshold were sorted visually online and then subsequently identified and isolated based on waveform similarity offline, using the OpenEx interface. Isolated single units had an SNR of at least 6 dB relative to the surrounding noise floor and stable waveform shapes. The acquired spikes were stored in data tank and analyzed using custom-written software in MATLAB.

Peristimulus time histograms were calculated by convolving an impulse vector generated from spike times with a Gaussian function with a standard deviation of 3 ms (Dayan and Abbott, 2001). Neural responses to the onset of the sound were investigated by calculating the mean firing rate for the 0–0.08 seconds time window. Wilcoxon's rank-sum test (MATLAB: ranksum) was used to test differences in sound-onset responses between age groups.

Investigation of neural synchronization was assessed using the normalized vector strength based on spike times (Herrmann et al., 2017). To this end, spike times (within the 0.08–0.225 seconds time window) were transformed to phase angles (p) using the following formula:

$$p = 2 f t \pi + \pi$$

where f is frequency and $\boldsymbol{t}$ a vector of spike times. Phase angles were wrapped to range from $-\pi$ to π. The empirical vector strength v (similar to ITPC described previously), that is, the resultant vector length, was calculated as follows (Lachaux et al., 1999):

$$v = \frac{1}{n}\left|\sum_{j=1}^{n} e^{ip_j}\right|$$

where v is the vector strength, i the imaginary unit, p the vector of phase angles, and n the number of spikes (with j being the index).

Vector strength can be biased by the number of spikes, with smaller v values for a higher number of spikes. To avoid biased estimates, a distribution of random vector strength values was calculated. That is, n (number of spikes) random phase values between $-\pi$ and π were generated and the vector strength (i.e., the resultant vector length) was calculated. Randomly drawing phase values and calculation of the vector strength was repeated 1000 times, which resulted in a distribution of random vector strengths given the number of spikes. The normalized vector strength was then calculated by subtracting the mean of the random vector strength distribution from the empirical vector strength and dividing the result by the standard deviation of the random vector strength distribution. The normalized vector strength was calculated for frequencies (f) ranging from 20 Hz to 180 Hz with a frequency resolution of 0.1 Hz, resulting in a vector strength spectrum. To test for differences in neural synchronization at the envelope frequency between age groups, the normalized vector strength was averaged across the 105–115 Hz frequencies. Wilcoxon's rank-sum test was used to test whether neural synchronization differed between age groups.

2.13. Effect size measure

Throughout the article, effect sizes are provided as r_e ($r_{equivalent}$; Rosenthal and Rubin, 2003). r_e is equivalent to a Pearson product-moment correlation for 2 continuous variables, to a point-biserial correlation for one continuous and one dichotomous variable and to the square root of partial η^2 for an analysis of variance.

3. Results

3.1. ABR amplitudes are reduced in aged animals

ABRs were recorded simultaneously from 2 electrode montages—one that emphasizes more caudal generators (putatively including the auditory nerve and the cochlear nucleus) and another that emphasizes more rostral generators (putatively including the inferior colliculus), as evidenced by the differences in ABR waveform morphology, modulation rate sensitivity, and the effects of anesthesia (Parthasarathy and Bartlett, 2012; Parthasarathy et al., 2014).

ABR wave 1 amplitudes were significantly decreased for aged compared with young rats (Fig. 2A, rostral channel: $p = 1.96^{e-4}$, $r_e = 0.701$, df = 21; caudal channel: $p = 7.20^{e-5}$, $r_e = 0.732$, df = 21). The wave 1 of the ABR originates in the auditory nerve, and its amplitude at suprathreshold sound levels is a physiological indicator for the degree of cochlear synaptopathy due to aging or noise exposure (Sergeyenko et al., 2013; Stamper and Johnson, 2015). This age-related decrease in ABR amplitudes was also observed for all subsequent waves (wave 3: $p = 5.55^{e-5}$, $r_e = 0.739$, df = 21; wave 4: $p = 9.92^{e-4}$, $r_e = 0.641$, df = 21; wave 5: $p = 7.17^{e-5}$, $r_e = 0.732$, df = 21; Fig. 2A) with generators in other brainstem and midbrain nuclei. Hence, there was an overall reduction in transient responses in the auditory nerve fibers, auditory brainstem, and midbrain with age.

3.2. Scalp-recorded neural synchronization shows strong spectral peaks and stimulus correlation with age despite weak ABR amplitudes

The ability of the auditory system to represent the various temporal regularities of speech were assessed using a measure of neural synchronization (i.e., EFR) evoked to the speech-like sound. The sensitivity of neural activity to the sound's temporal structure was assessed in 2 ways: cross-correlation and spectral amplitude (derived from an FFT). The overall temporal sensitivity was calculated by cross-correlating the time course of the scalp-recorded neural response with the stimulus time course. In the caudal channel, cross-correlation values were reduced for aged compared with young rats ($p = 1.96^{e-4}$, $r_e = 0.701$, df = 21) for the 300–3000

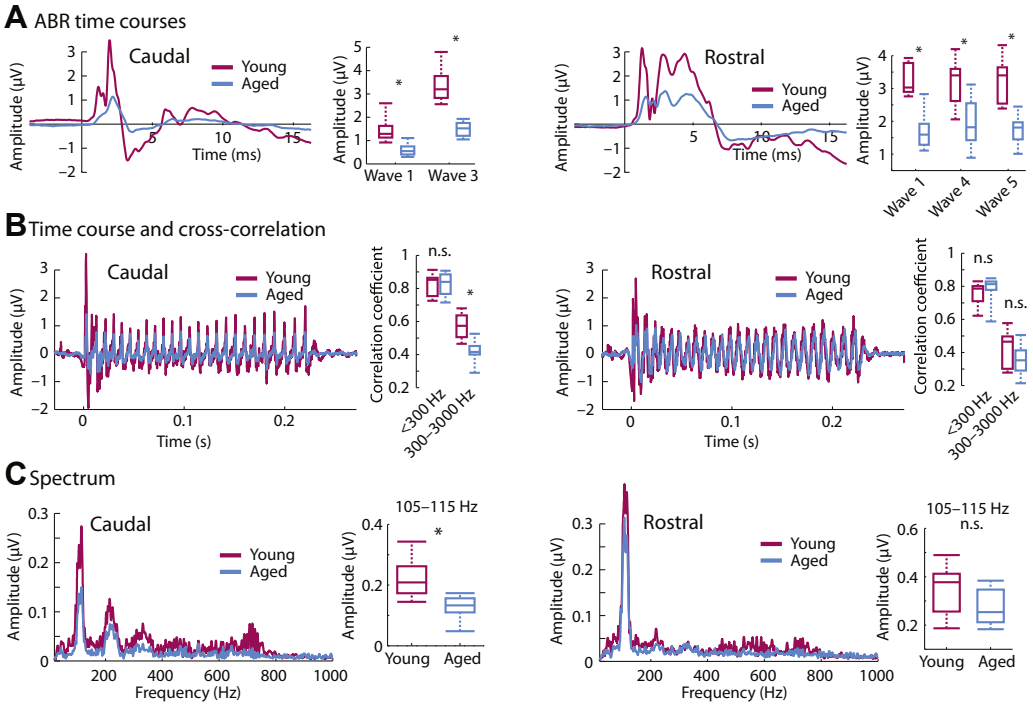

Fig. 2. Scalp-recorded potentials simultaneously recorded in 2 channels emphasizing rostral versus caudal generators. (A) Averaged click-evoked auditory brainstem responses (ABRs) and amplitudes for different ABR waves. (B) Time courses of envelope following responses (EFRs) in response to the speech-like /ba/ sound. Boxplots show coefficients from the cross-correlation for different frequency bands. (C) Amplitude spectra derived from fast Fourier transforms. Boxplots show neural synchronization strength to the sound's F0 envelope (105–115 Hz). $^*p < 0.05$. Abbreviation: n.s., not significant.

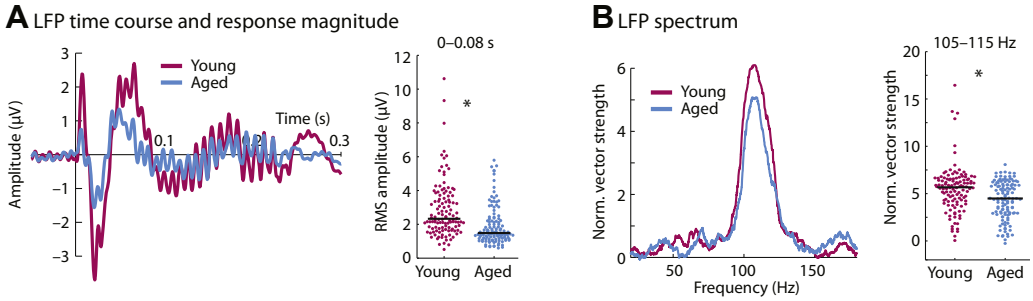

Fig. 3. Time course and spectrum for local field potentials. (A) Time course for each age group (left) and the root mean square (RMS) amplitude for the 0–0.08 seconds time window (right). (B) Spectrum of normalized vector strength (left) and the mean vector strength for the 105–115 Hz frequency window (right). In panels A and B, each dot reflects the normalized vector strength of an individual unit. The black horizontal line reflects the median across units. $^{*}p < 0.05$.

Hz frequency range that contains information about the sound's temporal fine structure. There was no difference in correlation values between young and aged animals for the <300-Hz frequency range (envelope) ($p = 0.878$, $r_e = 0.034$, df = 21; Fig. 2B, left). In the rostral channel with putative generators in the midbrain and its afferents, there was no age difference for the 300–3000 Hz frequency range ($p = 0.207$, $r_e = 0.273$, df = 21). However, aging was associated with an increase in correlation values for the <300 Hz range (envelope) although this was not significant ($p = 0.103$, $r_e = 0.349$, df = 21; Fig. 2B, right).

Spectral amplitudes derived via an FFT were averaged in the 105–115 Hz frequency band to assess neural synchronization to the temporal envelope (i.e., fundamental frequency; F0) of the speech-like sound. For the caudal channel, neural synchronization at the envelope frequency was larger for young compared with aged rats ($p = 5.06^{e-4}$, $r_e = 0.667$, df = 21; Fig. 2C, left). Although there was a similar trend in the rostral channel, this was not statistically significant ($p = 0.053$, $r_e = 0.409$, df = 21; Fig. 2C, right).

Taken together, our neural synchronization measures show that for caudal generators (auditory nerve, cochlear nucleus), synchronization was either similar or increased for younger compared with aged rats, whereas for rostral generators (lateral lemniscus, inferior colliculus), synchronization was similar for aged compared with younger rats. These data may suggest an age-related relative increase in synchronization strength along the ascending auditory pathway. Extracellular recordings from inferior colliculus neurons were obtained to further explore the age-related gain increases in the auditory system to the complex, speech-like sound.

3.3. LFP onset response and neural synchronization to the envelope are reduced in aged animals

Although changes in the neural representation of the speech-like sound were observed in the scalp-recorded synchronization measures, these EFRs reflect the superposition of activity from multiple generators. To localize age-related changes to the inferior colliculus and its afferents, we used LFPs as a proxy for the synaptic input to the inferior colliculus neurons. LFP time courses are displayed in Fig. 3A. Neural responses to the sound onset (RMS amplitude 0–0.08 seconds) was larger for young compared with aged animals ($p = 4.47^{e-9}$, $r_e = 0.368$, df = 237; Fig. 3A right), suggesting that the strength of the synaptic inputs to the inferior colliculus neurons decrease with age.

To investigate whether this decrease in synaptic input is accompanied by a decrease in LFP synchronization, the normalized vector strength at the F0 frequency (105–115 Hz) was measured in the sustained response of the LFP (0.08–0.225 seconds; Fig. 3B). Neural synchronization was larger for young compared with aged rats ($p = 2.66^{e-4}$, $r_e = 0.234$, df = 237). These results indicate that the synaptic inputs to the inferior colliculus neurons in response to a speech-like sound decrease in amplitude and synchrony with age.

3.4. Synchronization of multi-unit activity with the speech envelope are increased with age

To investigate the consequences of the age-related decrease in synaptic inputs (indicated by the LFPs) on the neural output of inferior colliculus neurons, multi-unit spiking activity was used as a proxy for neural population or network responses in the inferior colliculus. Time courses for the MUA are shown in Fig. 4. Spontaneous activity, quantified as the mean response in the time window preceding sound onset (−0.05 to 0 seconds), was larger in aged compared with young rats ($p = 2.91^{e-10}$, $r_e = 0.393$, df = 237; boxplots in Fig. 4A, left). Unlike the onset amplitudes of the LFPs (for which responses were reduced for aged animals), there was no difference in MUA neuronal responses to the sound onset (amplitude in the 0–0.08 seconds time window) between age groups ($p = 0.894$, re = 0.009, df = 237; Fig. 4A, middle and right).

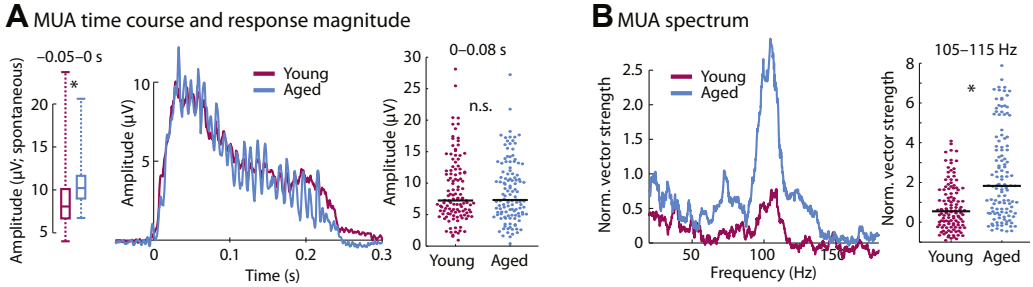

Fig. 4. Time course and spectrum for multi-unit activity. (A) left—the boxplots show the amplitude of the prestimulus onset time window (−0.05 to 0 seconds; i.e., spontaneous activity). Prestimulus onset activity was larger in aged compared with young animals ($p < 0.05$). Middle—time course for each age group (data are baseline corrected, i.e., the mean response in the −0.05 to 0 seconds time window was subtracted from the amplitude at each time point). Right—mean amplitude for the 0–0.08 seconds time window. (B) Spectrum of normalized vector strength (left) and the mean vector strength for the 105–115 Hz frequency window (right). In panels A and B, each dot reflects the normalized vector strength of an individual unit. The black horizontal line is the median across units. $^{*}p < 0.05$. Abbreviation: n.s., not significant.

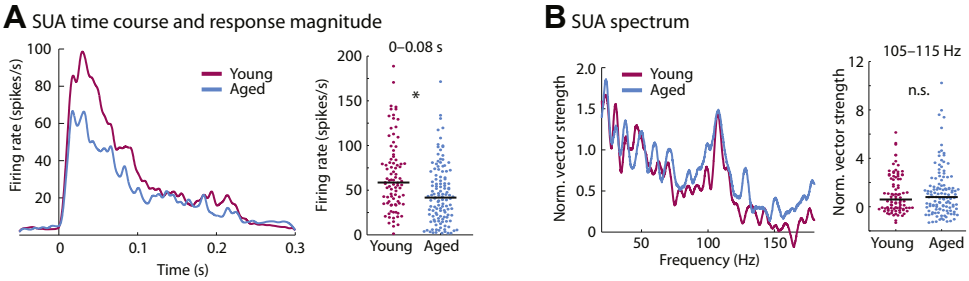

Fig. 5. Time course and spectrum for single-unit activity. (A) Peristimulus time histogram for each age group (left) and mean firing rate for the 0–0.08 seconds time window (right). (B) Spectrum of normalized vector strength (left) and the mean vector strength for the 105–115 Hz frequency window (right). In panels A and B, each dot reflects the normalized vector strength of an individual unit. The black horizontal line is the median across units. $^{*}p < 0.05$. Abbreviation: n.s., not significant.

Synchronization of MUA with the envelope of the sound was quantified using normalized vector strength (Fig. 4B). At the stimulation frequency (mean across the 105–115 Hz frequency window), neural synchronization was larger for aged compared with young rats ($p = 4.79^{e-9}$, $r_e = 0.367$, df = 237). Taken together, the LFP and MUA results suggest a relative increase in neural response and an increase in synchronization from a neuron's input to the neural population spiking output for aged compared with young animals.

3.5. Synchronization of single-unit activity with the speech envelope are similar between young and aged animals

Neuronal activity from well-isolated neurons (SUA) was analyzed to investigate whether individual neurons in the aged inferior colliculus also show a relative enhancement of onset-evoked activity and synchronization to the envelope.

Peristimulus time histograms for SUA are shown in Fig. 5. Spontaneous firing rates (i.e., in the −0.05 to 0 seconds time window) did not differ between age groups ($p = 0.831$, $r_e = 0.015$, df = 210). Firing rates to the sound onset (0–0.08 seconds) were larger for young compared with aged animals ($p = 1.02^{e-4}$, $r_e = 0.268$, df = 210; Fig. 5A). Neural synchronization to the envelope (F0) of the sound measured using normalized vector strength showed no effect of age (mean across the 105–115 Hz frequency window; $p = 0.703$, $r_e = 0.026$, df = 210; Fig. 5B). Given the reduced LFP synchronization, these results suggest an age-related increase in neural synchronization in SUA (a neuron's output) relative to the LFP (synaptic input), albeit to a lesser degree than for MUA.

3.6. Aging affects the relative change from LFP to spiking activity

To quantify the effects of aging on the relative changes from the LFP to spiking activity, we calculated the normalized difference between the LFP and SUA, and between the LFP and MUA. In detail, the LFP, SUA, and MUA were separately z-transformed by subtracting the mean and dividing by the standard deviation (including data points from young and aged rats). The z-transformation was separately calculated for onset responses (i.e., RMS or mean for the 0–0.08 seconds time window, for LFP and spiking activity, respectively) and neural synchronization (i.e., the mean normalized vector strength for the 105–115 Hz frequency window). For the LFP-to-SUA change, we subtracted the z-transformed LFP measure from the z-transformed SUA measure. The LFP-to-MUA change was calculated similarly by using the MUA instead of the SUA.

Wilcoxon's rank-sum test was used to test for differences between age groups (Fig. 6). For onset responses, there was no difference between age groups for the relative change from LFP to SUA ($p = 0.103$, $r_e = 0.115$, df = 202), but a significantly larger change from LFP to MUA in aged compared with young rats ($p = 1.47^{e-8}$, $r_e = 0.356$, df = 237). For neural synchronization, the change from LFP to SUA ($p = 0.018$, $r_e = 0.167$, df = 199) as well as the change from LFP to MUA ($p = 7.10^{e-12}$, $r_e = 0.425$, df = 237) was increased for aged compared with young rats.

3.7. Neural responses to a natural stimulus also show enhanced envelope sensitivity

To examine whether the observed effects using the noise carrier also translate to real speech, we additionally recorded neural activity in response to the original /ba/ speech-like sound using scalp-recorded EFRs and extracellular recordings for a subset of units in the inferior colliculus.

EFRs were obtained to a natural speech stimulus at 85 dB SPL for both young and aged animals in alternating polarities. The averaged waveforms were analyzed for responses to the envelope. A fixed sound level was used to account for the hearing thresholds of these rats at human speech frequencies, which are ~70 dB SPL at 1 kHz

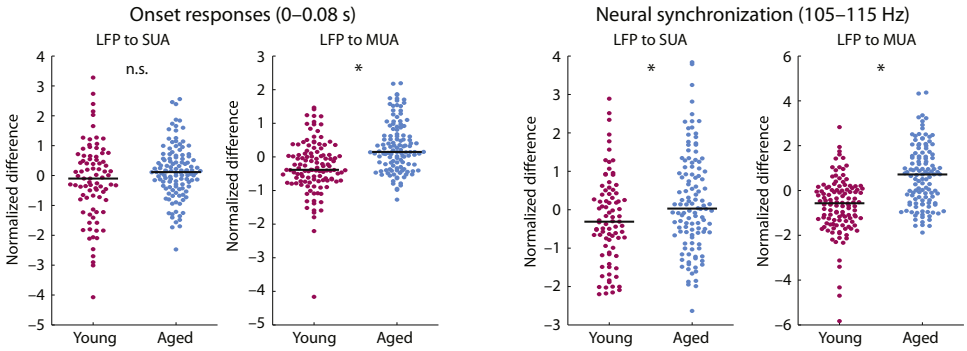

Fig. 6. Normalized difference between local field potential and spiking activity (SUA and MUA). Left: normalized difference for onset responses (time window from 0 to 0.08 seconds). Right: normalized difference for neural synchronization in the 0.08–0.225 seconds time window (frequency window from 105 to 115 Hz). Each dot reflects an individual unit. The black horizontal line is the median across units. $^{*}p < 0.05$. Abbreviations: MUA, multiunit activity; n.s., not significant; SUA, single-unit activity.

(Parthasarathy et al., 2014). The overall temporal sensitivity was calculated by cross-correlating the time course of the scalp-recorded neural response with the stimulus time course (Fig. 7A). In the caudal channel, cross-correlation values were reduced for aged compared with young rats ($p = 0.020$, $r_e = 0.527$, df = 17) for the <300-Hz frequency range that contains information about the sound's envelope (there was no such effect for the rostral channel: $p = 0.968$, $r_e = 0.010$, df = 17). There was no difference in correlation values between young and aged animals for the 300–3000 Hz frequency range (temporal fine structure) although cross-correlations tended to be higher in aged compared with young rats (caudal: $p = 0.051$, $r_e = 0.454$, df = 17; rostral: $p = 0.075$, $r_e = 0.417$, df = 17). Moreover, the amplitude spectrum of the EFRs was calculated for the rostral and caudal channel using an FFT (Fig. 7B). Neural synchronization to the envelope (105–115 Hz) was larger in young compared with aged rats (caudal: $p = 7.94^{e-4}$, $r_e = 0.703$, df = 17; rostral: $p = 2.65^{e-5}$, $r_e = 0.810$, df = 17). We also assessed the temporal fine structure responses by calculating the FFT on the difference wave between the two polarities with which the stimulus was presented. There was no difference between age groups in the spectrum for the 650–800 Hz frequency window (caudal: $p = 0.129$, $r_e = 0.361$, df = 17; rostral: $p = 0.904$, $r_e = 0.030$, df = 17).

Inferior colliculus neurons that were responsive to the /ba/ stimulus were found in lesser numbers compared with the speech-like sound due to the differences in the frequency sensitivity of the rat's hearing range. LFPs and MUA were recorded for 52 units in young animals and 20 units in aged animals. SUA was available for 33 units in young animals and 20 units in aged animals. The spectrum of normalized vector strength was calculated for LFPs, MUA, and SUA. The results are displayed in Fig. 7C and approximately mirror the results reported for the noise carrier. The effects of aging on neural synchronization to the stimulus envelope were assessed by comparing the mean normalized vector strength in the 105–115 Hz frequency window between age groups. For LFPs, there was no difference in neural synchronization between age groups ($p = 0.730$, $r_e = 0.042$, df = 70). An age-related increase in synchronization with the sound's envelope was observed for the MUA ($p = 9.78^{e-3}$, $r_e = 0.303$, df = 70). For SUA, there was no effect of age on neural synchronization to the envelope of the stimulus ($p = 0.345$, $r_e = 0.132$, df =51).

4. Discussion

In the present study, we used a systems-level (scalp recordings) and a microcircuit-level (LFPs and unit activity) approach to investigate the age-related changes in neural sensitivity to temporal regularity in a speech-like sound. Scalp-recorded potentials indicate that aging leads to a relative increase in neural synchronization to the periodicity envelope along the ascending auditory pathway. The underlying cellular changes in the midbrain were examined by recording neural activity from neurons in the inferior colliculus in response to the speech-like sound. We used the LFP as a proxy for a neuron's or neural population's synaptic inputs, and MUA and SUA as a measure of spiking output. LFP amplitudes to the sound onset and LFP neural synchronization to the temporal regularity of the envelope were smaller in aged compared with young

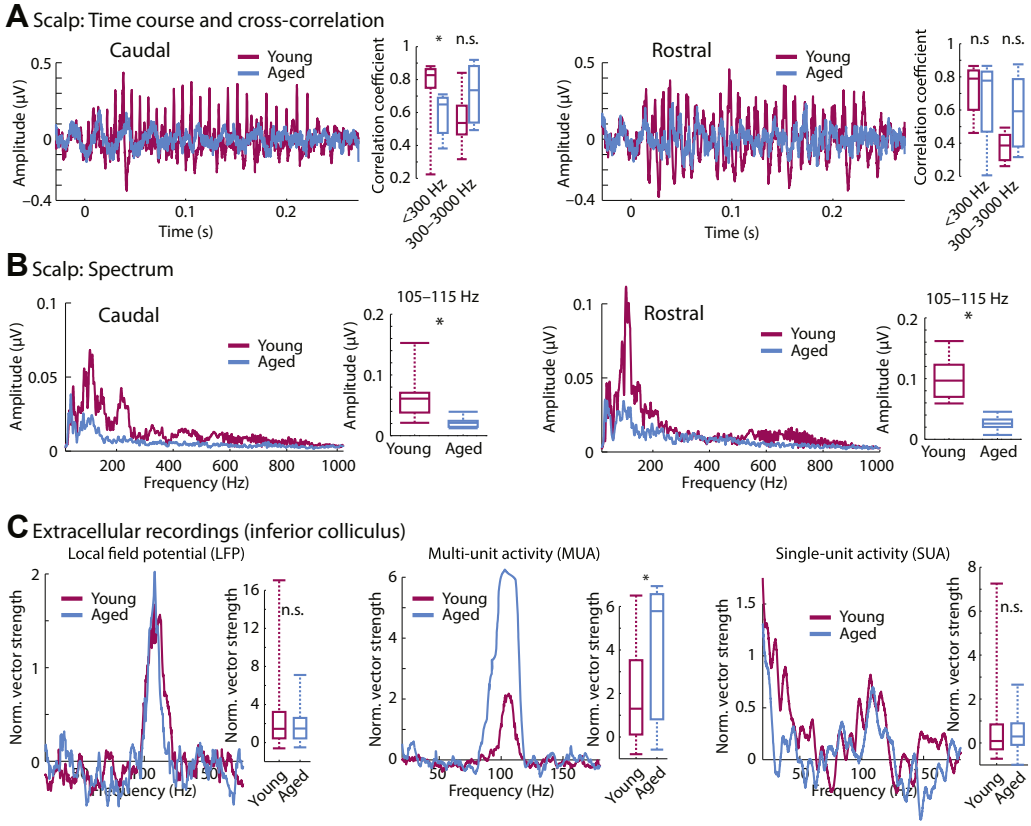

Fig. 7. Results for scalp recordings and extracellular recordings using a natural speech stimulus. (A) Time courses of envelope following responses (EFRs) in response to the speech /ba/ sound. Boxplots show coefficients from the cross-correlation for different frequency bands. (B) Amplitude spectra derived from fast Fourier transforms. Boxplots show neural synchronization strength to the sound's F0 envelope (105–115 Hz). (C) Spectrum of normalized vector strength for LFPs, MUA, and SUA in response to the speech sound. Boxplots show the mean normalized vector strength for the 105–115 Hz frequency window. *$p < 0.05$. Abbreviations: LFPs, local field potentials; MUA, multiunit activity; n.s., not significant; SUA, single-unit activity.

rats. By contrast, MUA and, to a lesser degree, SUA showed an aged-related relative increase in synchronization to the periodicity envelope. Our results suggest that aging is associated with altered sensitivity to sounds and a sound's temporal regularities, and that these effects may be due to altered gain in neural network activity in the aged auditory midbrain.

4.1. Scalp-evoked potentials point to a decrease in brainstem responses and an increase in inferior colliculus responses

Auditory brainstem responses (ABRs) and neural synchronization (i.e., EFRs) have been used to study age-related changes in neural activity to speech and other complex sounds in humans (Anderson et al., 2012; Clinard and Tremblay, 2013; Stamper and Johnson, 2015). The ability to obtain these responses non-invasively makes them an ideal bridge between human studies and studies in animal models, for which the underlying pathophysiology can additionally be studied at the microcircuit level using more invasive techniques (Shaheen et al., 2015; Zhong et al., 2014).

Consistent with previous studies (Fernandez et al., 2015; Parthasarathy et al., 2014; Parthasarathy and Kujawa, 2018; Sergeyenko et al., 2013), we observed an age-related decrease in the wave 1 amplitude of the ABR to clicks at suprathreshold sound levels (Fig. 2A). The wave 1 of the ABR at suprathreshold sound levels may be considered as a physiological indicator for the degree of cochlear synaptopathy, that is, the loss of synapses between the inner hair cells and the auditory nerve fibers (Konrad-Martin et al., 2012; Kujawa and Liberman, 2009). This cochlear synaptopathy has been observed in aging and noise-exposed animals, including mice (Fernandez et al., 2015; Parthasarathy and Kujawa, 2018; Sergeyenko et al., 2013), rats (Mohrle et al., 2016), gerbils (Gleich et al., 2016), guinea pigs (Furman et al., 2013; Schmeidt et al., 1996), and macaques (Valero et al., 2017), in addition to the evidence from postmortem human temporal bones (Viana et al., 2015). The reduction of wave 1 in aged compared with young rats thus suggests the presence of cochlear synaptopathy in the aged population used in the present study.

The sensitivity of the scalp-recorded EFRs to regular temporal structure in a speech-like sound was investigated using measures of neural synchronization. We observed reduced synchronization to the envelope and fine structure information for activity likely originating in the auditory nerve and cochlear nucleus (Fig. 2, left). Signals likely originating from rostral generators, including the inferior colliculus, showed an age-related increase in neural synchronization to the envelope of the speech-like sound (Fig. 2B and C). These results suggest an age-related transformation in the neural representation of envelope cues in speech along the ascending auditory pathway, which we investigated further using more invasive extracellular electrophysiological methods.

4.2. Aging increases network-level activity of inferior colliculus neurons relative to their synaptic inputs

To study the contributions of the auditory midbrain to the changes seen in the scalp-recorded responses, we simultaneously recorded LFPs and unit responses from the same site in response to sound. LFPs are thought to be largely the aggregate presynaptic activity at the dendrites and the soma, and hence a proxy for the inputs to the neuron or neuronal region (Buzsaki et al., 2012; Gourevitch and Edeline, 2011; Logothetis et al., 2001; Logothetis and Wandell, 2004). By comparing these LFPs to the spiking output, the transformation of these sound representations in the inferior colliculus can be investigated (Herrmann et al., 2017).

In the present study, LFPs to the sound onset and neural synchronization to the sound's envelope were decreased for aged compared with young rats (Fig. 3), suggesting that inputs to the inferior colliculus neurons are degraded. By contrast, multi-unit spiking activity in the inferior colliculus—reflecting population or network output—revealed no age difference in the onset response and age-related increase in synchronization to the sound's envelope (Fig. 4). This relative enhancement seen at the population level (MUA) was also present, albeit to a lesser degree, at the level of the single neurons (SUA, Figs. 5 and 6). These results suggest that the inferior colliculus neurons selectively increase their neuronal activity to the envelope of a speech-like sound in aged animals, despite the reduced synaptic inputs to these neurons.

Previous work suggested that midbrain neurons responding to simple stimuli such as tones and noise bursts show remarkably subtle changes with age (Willott et al., 1988a,b). This is despite the extensive degradation of the peripheral auditory system, such as the loss of outer hair cells (Chen et al., 2009; Spongr et al., 1997), changes in endocochlear potential (Ohlemiller et al., 2006), and the loss of cochlear synapses (Sergeyenko et al., 2013) and spiral ganglion neurons in the auditory nerve (Bao and Ohlemiller, 2010). Even when studies using single-unit recordings do find age-related changes in temporal processing (Palombi et al., 2001; Walton et al., 2002), it is unclear whether these changes are inherited from previous stages of auditory processing, or generated in the nucleus being studied. Our approach in this study shows that the enhancements seen in the spiking output of the inferior colliculus neurons, in particular at the population and network level, may explain some of this dichotomy in peripheral versus central responses with age.

4.3. Potential mechanisms underlying age-related changes in sensitivity to temporal regularity in sounds

Acute insults (e.g., ototoxic drugs or mechanical deafening) to the auditory system damage the auditory periphery and trigger homeostatic changes in the auditory pathway (Chambers et al., 2016; Kotak et al., 2005). The most drastic change reported is the loss of inhibitory circuits and function (Caspary et al., 2013; Ling et al., 2005; Resnik and Polley, 2017; Richardson et al., 2013), which, in turn, increases neuronal activity in the central auditory structures (Chambers et al., 2016). The effects of age on the auditory system may occur along with other forms of hearing loss. In fact, it is a current debate whether hearing deficits entirely due to aging even exist (Humes et al., 2012). In the present study, the Fischer-344 rat is known to exhibit metabolic and high-frequency hearing loss (Syka, 2010). We have minimized the contributions of peripheral threshold elevations by normalizing the presentation level for each animal. However, other aspects of peripheral hearing loss, such as cochlear synaptopathy may still contribute to a decreased peripheral drive with age. The current data in combination with recent evidence suggest that central auditory systems undergo gain increases similar to acute hearing loss, when the peripheral insult is gradual as is the case for aging (Lai et al., 2017; Parthasarathy et al., 2014; Parthasarathy and Kujawa, 2018; Presacco et al., 2016).

The increase in neuronal activity due to a loss of inhibition is typically accompanied by a reduction in the precision of neural coding. Inferior colliculus neurons change their tuning curves to become less selective with age (Leong et al., 2011; Rabang et al., 2012). In addition, sensitivity to temporal regularities in simple stimuli increases for slow amplitude modulations but decreases for fast amplitude modulations in aged animals (Herrmann et al., 2017; Walton et al., 2002). In the present study, inferior colliculus neurons in aged animals showed an increase in the spontaneous firing rate (Fig. 4A), which suggests inhibition was reduced in the aged midbrain. Furthermore, despite reduced synaptic inputs to inferior colliculus neurons (as indexed by our LFP recordings), neuronal

firing of populations of inferior colliculus neurons was overly synchronized with the envelope of a speech-like sound in aged compared with young animals (Figs. 3 and 4). Our data thus suggest that temporal response precision is altered in the aged midbrain due to hypersensitivity in networks of neurons.

Increased gain in the auditory system may lead to better detection of weak signals in neural circuits, and may, in turn, support hearing in quiet environments (Chambers et al., 2016). For example, hearing loss has been shown to increase sensitivity to suprathreshold amplitude modulation in sounds (Moore et al., 1996). However, neural gain enhancements may come at the cost of poor discrimination between stimuli (Guo et al., 2017). For example, discrimination between fundamental frequency in speech is reduced for older adults with clinically normal audiograms (Vongpoisal and Pichora-Fuller, 2007), and a gain increase in cortex has been linked to poor speech perception in the presence of competing sound (Millman et al., 2017). Hence, an aberrant neural gain increase in aging may not be beneficial for listening to sounds that are typical of everyday life, such as speech, when perception requires the segregation of different concurrent sounds.

5. Conclusions

We investigated how aging affects neural sensitivity to temporal regularity in a speech-like sound. Systems level recordings (i.e., at the scalp) were combined with microcircuit recordings (i.e., LFPs and unit activity recorded extracellularly) in young and aged rats. We show that aging is associated with increased neural activity along the ascending auditory pathway, which alters the sensitivity of midbrain (i.e., inferior colliculus) neurons to temporally regular structure in sounds. Specifically, synchronization to the periodicity envelope in speech (at the fundamental frequency) was enhanced for spiking activity of populations of inferior colliculus neurons in aged rats, despite the neuron's reduced synaptic input. The data suggest that temporal response precision is altered in the aged midbrain due to hypersensitivity in networks of neurons.

Disclosure statement

The authors declare no competing conflicts of interest.

Acknowledgements

This study was supported by NIDCD DC-011580 to ELB. BH was supported by the Canada First Research Excellence Fund BrainsCAN postdoctoral fellowship.

References

Allen, P.D., Eddins, D.A., 2010. Presbycusis phenotypes form a heterogeneous continuum when ordered by degree and configuration of hearing loss. Hear. Res. 264, 10–20.
Anderson, S., Parbery-Clark, A., White-Schwoch, T., Kraus, N., 2012. Aging affects neural precision of speech encoding. J. Neurosci. 32, 14156–14164.
Anderson, S., Parbery-Clark, A., Yi, H.-G., Kraus, N., 2011. A neural basis of speech-in-noise perception in older adults. Ear Hear. 32, 750–757.
Bao, J.X., Ohlemiller, K.K., 2010. Age-related loss of spiral ganglion neurons. Hear. Res. 264, 93–97.
Bregman, A.S., 1990. Auditory Scene Analysis; the Perceptual Organization of Sound. MIT Press, Cambridge, MA.
Bullock, T.H., 1997. Signals and signs in the nervous system: the dynamic anatomy of electrical activity is probably information-rich. Proc. Natl. Acad. Sci. U. S. A. 94, 1–6.
Buzsaki, G., Anastassiou, C.A., Koch, C., 2012. The origin of extracellular fields and currents - EEG, ECoG, LFP and spikes. Nat. Rev. Neurosci. 13, 407–420.
Caspary, D.M., Hughes, L.F., Ling, L.L., 2013. Age-related GABA(A) receptor changes in rat auditory cortex. Neurobiol. Aging 34, 1486–1496.
Caspary, D.M., Ling, L., Turner, J.G., Hughes, L.F., 2008. Inhibitory neurotransmission, plasticity and aging in the mammalian central auditory system. J. Exp. Biol. 211, 1781–1791.
Chambers, A.R., Resnik, J., Yuan, Y.S., Whitton, J.P., Edge, A.S., Liberman, M.C., Polley, D.B., 2016. Central gain restores auditory processing following near-complete cochlear denervation. Neuron 89, 867–879.
Chen, G.D., Li, M.N., Tanaka, C., Bielefeld, E.C., Hu, B.H., Kermany, M.H., Salvi, R., Henderson, D., 2009. Aging outer hair cells (OHCs) in the Fischer 344 rat cochlea: function and morphology. Hear. Res. 248, 39–47.
Clinard, C.G., Tremblay, K.L., 2013. Aging degrades the neural encoding of simple and complex sounds in the human brainstem. J. Am. Acad. Audiol. 24, 590–599.
Dayan, P., Abbott, L.F., 2001. Theoretical Neuroscience: Computational and Mathematical Modeling of Neural Systems. MIT Press, Cambridge, MA.
Drummond, G.B., 2009. Reporting ethical matters in the Journal of Physiology: standards and advice. J. Physiol. 587, 713–719.
Dubno, J.R., Eckert, M.A., Lee, F.S., Matthews, L.J., Schmiedt, R.A., 2013. Classifying human audiometric phenotypes of age-related hearing loss from animal models. J. Assoc. Res. Otolaryngol. 14, 687–701.
Fernandez, K.A., Jeffers, P.W.C., Lall, K., Liberman, M.C., Kujawa, S.G., 2015. Aging after noise exposure: acceleration of cochlear synaptopathy in "recovered" ears. J. Neurosci. 35, 7509–7520.
Frisina, D.R., Frisina, R.D., 1997. Speech recognition in noise and presbycusis: Relations to possible neural mechanisms. Hear. Res. 106, 95–104.
Fullgrabe, C., Moore, B.C.J., Stone, M.A., 2015. Age-group differences in speech identification despite matched audiometrically normal hearing: contributions from auditory temporal processing and cognition. Front Aging Neurosci. 6, 347.
Furman, A.C., Kujawa, S.G., Liberman, M.C., 2013. Noise-induced cochlear neuropathy is selective for fibers with low spontaneous rates. J. Neurophysiol. 110, 577–586.
Gao, F., Berrebi, A.S., 2016. Forward masking in the medial nucleus of the trapezoid body of the rat. Brain Struct. Funct. 221, 2303–2317.
Gleich, O., Semmler, P., Strutz, J., 2016. Behavioral auditory thresholds and loss of ribbon synapses at inner hair cells in aged gerbils. Exp. Gerontol. 84, 61–70.
Gordon-Salant, S., Fitzgibbons, P.J., 2001. Sources of age-related recognition difficulty for time-compressed speech. J. Speech Lang. Hear. Res. 44, 709–719.
Gourevitch, B., Edeline, J.M., 2011. Age-related changes in the Guinea pig auditory cortex: relationship with brainstem changes and comparison with tone-induced hearing loss. Eur. J. Neurosci. 34, 1953–1965.
Guo, W., Clause, A.R., Barth-Maron, A., Polley, D.B., 2017. A corticothalamic circuit for dynamic switching between feature detection and discrimination. Neuron 95, 180–194.
Herrmann, B., Parthasarathy, A., Bartlett, E.L., 2017. Ageing affects dual encoding of periodicity and envelope shape in rat inferior colliculus neurons. Eur. J. Neurosci. 45, 299–311.
Herrmann, B., Parthasarathy, A., Han, E.X., Obleser, J., Bartlett, E.L., 2015. Sensitivity of rat inferior colliculus neurons to frequency distributions. J. Neurophysiol. 114, 2941–2954.
Hughes, L.F., Turner, J.G., Parrish, J.L., Caspary, D.M., 2010. Processing of broadband stimuli across A1 layers in young and aged rats. Hear. Res. 264, 79–85.
Humes, L.E., Dubno, J.R., Gordon-Salant, S., Lister, J.J., Cacace, A.T., Cruickshanks, K.J., Gates, G.A., Wilson, R.H., Wingfield, A., 2012. Central presbycusis: a review and evaluation of the evidence. J. Am. Acad. Audiol. 23, 635–666.
Ingham, N.J., Itatani, N., Bleeck, S., Winter, I.M., 2016. Enhancement of forward suppression begins in the ventral cochlear nucleus. Brain Res. 1639, 13–27.
Konrad-Martin, D., Dille, M.F., McMillan, G., Griest, S., McDermott, D., Fausti, S.A., Austin, D.F., 2012. Age-related changes in the auditory brainstem response. J. Am. Acad. Audiol. 23, 18–35.
Kotak, V.C., Fujisawa, S., Lee, F.A., Karthikeyan, O., Aoki, C., Sanes, D.H., 2005. Hearing loss raises excitability in the auditory cortex. J. Neurosci. 25, 3908–3918.
Kujawa, S.G., Liberman, M.C., 2009. Adding insult to injury: cochlear nerve degeneration after "temporary" noise-induced hearing loss. J. Neurosci. 29, 14077–14085.
Lachaux, J.-P., Rodriguez, E., Martinerie, J., Varela, F.J., 1999. Measuring phase synchrony in brain signals. Hum. Brain Mapp. 8, 194–208.
Lai, J., Sommer, A.L., Bartlett, E.L., 2017. Age-related changes in envelope-following responses at equalized peripheral or central activation. Neurobiol. Aging 58, 191–200.
Lakatos, P., Musacchia, G., O'Connel, M.N., Falchier, A.Y., Javitt, D.C., Schroeder, C.E., 2013. The spectrotemporal filter mechanism of auditory selective attention. Neuron 77, 750–761.
Lakatos, P., Shah, A.S., Knuth, K.H., Ulbert, I., Karmos, G., Schroeder, C.E., 2005. An oscillatory hierarchy controlling neuronal excitability and stimulus processing in the auditory cortex. J. Neurophysiol. 94, 1904–1911.
Leong, U.C., Barsz, K., Allen, P.D., Walton, J.P., 2011. Neural correlates of age-related declines in frequency selectivity in the auditory midbrain. Neurobiol. Aging 32, 168–178.
Ling, L.L., Hughes, L.F., Caspary, D.M., 2005. Age-related loss of the GABA synthetic enzyme glutamic acid decarboxylase in rat primary auditory cortex. Neuroscience 132, 1103–1113.
Logothetis, N.K., Pauls, J., Augath, M., Trinath, T., Oeltermann, A., 2001. Neurophysiological investigation of the basis of the fMRI signal. Nature 412, 150–157.
Logothetis, N.K., Wandell, B.A., 2004. Interpreting the BOLD signal. Annu. Rev. Physiol. 66, 735–769.
Millman, R.E., Mattys, S.L., Gouws, A.D., Prendergast, G., 2017. Magnified neural envelope coding predicts deficits in speech perception in noise. J. Neurosci. 37, 7727–7736.
Mohrle, D., Ni, K., Varakina, K., Bing, D., Lee, S.C., Zimmermann, U., Knipper, M., Ruttiger, L., 2016. Loss of auditory sensitivity from inner hair cell synaptopathy

can be centrally compensated in the young but not old brain. Neurobiol. Aging 44, 173–184.
Moore, B.C.J., Wojtczak, M., Vickers, D.A., 1996. Effect of loudness recruitment oil the perception of amplitude modulation. J. Acoust. Soc. Am. 100, 481–489.
Ohlemiller, K.K., Lett, J.M., Gagnon, P.M., 2006. Cellular correlates of age-related endocochlear potential reduction in a mouse model. Hear. Res. 220, 10–26.
Palombi, P.S., Backoff, P.M., Caspary, D.M., 2001. Responses of young and aged rat inferior colliculus neurons to sinusoidally amplitude modulated stimuli. Hear. Res. 153, 174–180.
Parthasarathy, A., Bartlett, E., 2012. Two-channel recording of auditory-evoked potentials to detect age-related deficits in temporal processing. Hear. Res. 289, 52–62.
Parthasarathy, A., Datta, J., Torres, J.A.L., Hopkins, C., Bartlett, E.L., 2014. Age-related changes in the relationship between auditory brainstem responses and envelope-following responses. J. Assoc. Res. Otolaryngol. 15, 649–661.
Parthasarathy, A., Lai, J., Bartlett, E.L., 2016. Age-related changes in processing simultaneous amplitude modulated sounds assessed using envelope following responses. J. Assoc. Res. Otolaryngol. 17, 119–132.
Parthasarathy, A., Kujawa, S.G., 2018. Synaptopathy in the aging cochlea: characterizing early-neural deficits in auditory temporal envelope processing. J. Neurosci. 38, 7108–7119.
Paxinos, G., Watson, C., 2006. The Rat Brain in Stereotaxic Coordinates. Academic Press, Cambridge, MA.
Pichora-Fuller, M.K., Souza, P.E., 2001. Effects of Aging on Auditory Processing of Speech. Workshop on Candidature for and Delivery of Audiological Services - Special Needs of Older People. B C Decker Inc, Eriksholm, Denmark, pp. S11–S16.
Presacco, A., Simon, J.Z., Anderson, S., 2016. Evidence of degraded representation of speech in noise, in the aging midbrain and cortex. J. Neurophysiol. 116, 2346–2355.
Rabang, C.F., Parthasarathy, A., Venkataraman, Y., Fisher, Z.L., Gardner, S.M., Bartlett, E.L., 2012. A computational model of inferior colliculus responses to amplitude modulated sounds in young and aged rats. Front Neural Circuits 6, 77.
Resnik, J., Polley, D.B., 2017. Fast-spiking GABA circuit dynamics in the auditory cortex predict recovery of sensory processing following peripheral nerve damage. Elife 6, e21452.
Richardson, B.D., Ling, L.L., Uteshev, V.V., Caspary, D.M., 2013. Reduced GABA(A) receptor-mediated tonic inhibition in aged rat auditory thalamus. J. Neurosci. 33, 1218, 27a.
Rosen, S., 1992. Temporal information in speech - acoustic, auditory and linguistic aspects. Philos. Trans. R. Soc. Lond. B Biol. Sci. 336, 367–373.
Rosenthal, R., Rubin, D.B., 2003. Requivalent: a simple effect size indicator. Psychol. Methods 8, 492–496.
Ruggles, D., Bharadwaj, H., Shinn-Cunningham, B.G., 2011. Normal hearing is not enough to guarantee robust encoding of suprathreshold features important in everyday communication. Proc. Natl. Acad. Sci. U S A. 108, 15516–15521.
Schatteman, T.A., Hughes, L.F., Caspary, D.M., 2008. Aged-related loss of temporal processing: altered responses to amplitude modulated tones in rat dorsal cochlear nucleus. Neuroscience 154, 329–337.
Schmiedt, R.A., Mills, J.H., Boettcher, F.A., 1996. Age-related loss of activity of auditory-nerve fibers. J. Neurophysiol. 76, 2799–2803.
Schoof, T., Rosen, S., 2016. The role of age-related declines in subcortical auditory processing in speech perception in noise. J. Assoc. Res. Otolaryngol. 17, 441–460.
Sergeyenko, Y., Lall, K., Liberman, M.C., Kujawa, S.G., 2013. Age-related cochlear synaptopathy: an early-onset contributor to auditory functional decline. J. Neurosci. 33, 13686–13694.
Shaheen, L.A., Valero, M.D., Liberman, M.C., 2015. Towards a diagnosis of cochlear neuropathy with envelope following responses. J. Assoc. Res. Otolaryngol. 16, 727–745.
Snyder, R.L., Schreiner, C.E., 1985. Forward masking of the auditory-nerve neurophonic (ann) and the frequency following response (FFR). Hearing Res. 20, 45–62.
Spongr, V.P., Flood, D.G., Frisina, R.D., Salvi, R.J., 1997. Quantitative measures of hair cell loss in CBA and C57BL/6 mice throughout their life spans. J. Acoust. Soc. Am. 101, 3546–3553.
Stamper, G.C., Johnson, T.A., 2015. Auditory function in normal-hearing, noise-exposed human ears. Ear Hear. 36, 172–184.
Syka, J., 2010. The Fischer 344 rat as a model of presbycusis. Hear. Res. 264, 70–78.
Takesian, A.E., Kotak, V.C., Sanes, D.H., 2009. Developmental Hearing loss disrupts synaptic inhibition: implications for auditory processing. Future Neurol. 4, 331–349.
Valero, M.D., Burton, J.A., Hauser, S.N., Hackett, T.A., Ramachandran, R., Liberman, M.C., 2017. Noise-induced cochlear synaptopathy in rhesus monkeys (Macaca mulatta). Hearing Res. 353, 213–223.
Verschooten, E., Robles, L., Kovacic, D., Joris, P.X., 2012. Auditory nerve frequency tuning measured with forward-masked compound action potentials. J. Assoc. Res. Otolaryngol. 13, 799–817.
Viana, L.M., O'Malley, J.T., Burgess, B.J., Jones, D.D., Oliveira, C., Santos, F., Merchant, S.N., Liberman, L.D., Liberman, M.C., 2015. Cochlear neuropathy in human presbycusis: Confocal analysis of hidden hearing loss in post-mortem tissue. Hear. Res. 327, 78–88.
Vongpoisal, T., Pichora-Fuller, M.K., 2007. Effect of age on F-0 difference limen and concurrent vowel identification. J. Speech Lang. Hear. Res. 50, 1139–1156.
Walton, J.P., 2010. Timing is everything: temporal processing deficits in the aged auditory brainstem. Hear. Res. 264, 63–69.
Walton, J.P., Frisina, R.D., O'Neill, W.E., 1998. Age-related alteration in processing of temporal sound features in the auditory midbrain of the CBA mouse. J. Neurosci. 18, 2764–2776.
Walton, J.P., Simon, H., Frisina, R.D., 2002. Age-related alterations in the neural coding of envelope periodicities. J. Neurophysiol. 88, 565–578.
Willott, J.F., Parham, K., Hunter, K.P., 1988a. Response properties of inferior colliculus neurons in middle-aged C57bl/6J mice with presbycusis. Hear. Res. 37, 15–27.
Willott, J.F., Parham, K., Hunter, K.P., 1988b. Response properties of inferior colliculus neurons in young and very old CBa/J mice. Hear. Res. 37, 1–14.
Wolff, M.J., Jochim, J., Akyürek, E.G., Stokes, M.G., 2017. Dynamic hidden states underlying working-memory-guided behavior. Nat. Neurosci. 20, 864–871.
Zhong, Z.W., Henry, K.S., Heinz, M.G., 2014. Sensorineural hearing loss amplifies neural coding of envelope information in the central auditory system of chinchillas. Hear. Res. 309, 55–62.